Title

High-throughput screening of FDA-approved drugs using oxygen biosensor plates reveals secondary mitofunctional effects

Authors

Sahdeo, Sunil
Tomilov, Alexey
Komachi, Kelly
et al.

Publication Date

2014-07-01

DOI

10.1016/j.mito.2014.07.002

Peer reviewed

Published in final edited form as:
Mitochondrion. 2014 July ; 17: 116–125. doi:10.1016/j.mito.2014.07.002.

High-throughput screening of FDA-approved drugs using oxygen biosensor plates reveals secondary mitofunctional effects

Sunil Sahdeo[a], **Alexey Tomilov**[a], **Kelly Komachi**[c], **Christine Iwahashi**[b], **Sandipan Datta**[a], **Owen Hughes**[c], **Paul Hagerman**[b], and **Gino Cortopassi**[a]

[a]Department of Molecular Biosciences, School of Veterinary Medicine, University of California, Davis, 1089 Veterinary Medicine Drive, Davis, CA, 95616

[b]Department of Biochemistry and Molecular Medicine, School of Medicine, University of California, Davis, 4455 Tupper Hall, Davis, CA, 95616

[c]Eon Research, 707 4th Street, Suite 305, Davis, CA 95616

Abstract

Repurposing of FDA-approved drugs with effects on mitochondrial function might shorten the critical path to mitochondrial disease drug development. We improved a biosensor-based assay of mitochondrial O_2 consumption, and identified mitofunctional defects in cell models of LHON and FXTAS. Using this platform, we screened a 1600-compound library of clinically used drugs. The assay identified drugs known to affect mitochondrial function, such as metformin and decoquinate. We also identified several drugs not previously known to affect mitochondrial respiration including acarbose, metaraminol, gallamine triethiodide, and acamprosate. These previously unknown 'mitoactives' represent novel links to targets for mitochondrial regulation and potentially therapy, for mitochondrial disease.

Keywords

Mitochondrial disease; Oxygen; Bioenergetics; Biosensor; Repurposing; Orphan; High-throughput screening

1. Introduction

Mitochondria play critical roles in a number of cellular processes including energy production, biosynthesis, and apoptosis. Drugs that increase mitochondrial function could potentially find applications in treating metabolic disorders, aiding recovery from injury or

Corresponding Author: Gino Cortopassi Professor Department of Molecular Biosciences School of Veterinary Medicine, University of California, Davis 1089 Veterinary Medicine Drive. Davis, CA, 95616 (530)754-9665.

illness or delay aging. Mitochondrial dysfunction occurs in a number of rare diseases (LHON, Leigh's Syndrome, Friedreich's ataxia, FXTAS)(Goto et al., 1992; Kaplan, 1999; Ross-Inta et al., 2010; Santorelli et al., 1993; Shoffner et al., 1990; Wallace et al., 1988), as well as more common neurodegenerative diseases (Alzheimer's, Parkinson's and Amyotrophic lateral sclerosis)(Hirai et al., 2001; Schapira et al., 1990; Wallace, 1999; Wong et al., 1995). Agents that increase mitochondrial function or number could potentially provide therapies for these indications.

Currently, however, there are no FDA approved 'mitochondrial therapeutics' (Armstrong, 2007; Toogood, 2008). One strategy for finding such drugs is to screen for drugs that modify mitochondrial function. Since mitochondrial activity is responsible for virtually all oxygen use by the cell, oxygen consumption is a reliable indicator of mitochondrial activity. The traditional 'gold standard' for measuring mitochondrial function utilizes the Clark-type oxygen electrode. Although accurate, it is time-intensive and not ideal for high-throughput screening. Previously we validated 96-well oxygen Biosensor plates as a means of monitoring positive or negative effectors of mitochondrial oxygen consumption (Rolo et al., 2009). Here we demonstrate new optimized conditions in a 384-well format that is amenable to high throughput.

For validation, using biosensor plates we screened a small library of 1600 drugs that have been FDA approved or clinically evaluated. We identified potentiators of oxygen consumption at a criterion of plus or minus 2 standard deviations from the control mean, with a 3-6% hit rate. Inhibitors of mitochondrial function were identified with a similar hit rate of between 2-3%. We followed up multiple hits and generated dose response curves. The assay accurately detected known mitochondrial inhibitors, such as metformin. Several of the drugs that positively affect mitochondrial function could be considered as leads to try to boost mitochondrial function in the context of an inherited deficiency. Among the drugs that inhibit mitochondrial function, some inhibit only mildly and may have beneficial metabolic effects, possibly through the induction of AMP-activated protein kinase (AMPK). Taken together, this assay platform has the potential to rapidly screen drugs/candidate molecules for both mitochondrial stimulation and mitochondrial toxicity in a high-throughput mode.

2. Materials and Methods

2. 1 Cell lines and cell culture

RGC-5 cells and LHON cybrids were kindly provided by Dr. Neeraj Agarwal and Dr. Valerio Carelli respectively. FXTAS dermal fibroblasts were generated at UC Davis and described previously (Ross-Inta et al., 2010). All other cell lines were purchased from American Type Culture Collection (Manassas, VA) or Coriell Cell Repositories (Camden, NJ) and grown in a humidified atmosphere containing 5% CO_2 at 37°C. Fibroblasts and lymphoblasts were grown in minimal essential medium (MEM; Life Technologies, Gaithersburg, MD), supplemented with 8 mM glutamine, 10% fetal bovine serum (FBS), 50 μg/ml uridine, 1 mM sodium pyruvate, 10 μg/ml insulin, 10 ng/ml epidermal growth factor (EGF), 50 ng/ml basic growth factor, and gentamicin. 3T3 and C2C12 cells were grown in DMEM supplemented with 2 mM glutamine and 10% FBS. 50B11 cells were grown in

Neurobasal media supplemented with 2 mM glutamine, B-27 supplement and 10% FBS. K562 cells were grown in RPMI medium supplemented with 10% FBS. FL83B cells were grown in F12 medium supplemented with 10% FBS. RGC-5 cells were grown in DMEM supplemented with 2 mM glutamine, 50 μg/ml uridine, and 10% FBS. All cell types were evaluated in the same assay buffer (phenol-red DMEM supplemented with 1 mM Na Pyruvate and 10% FBS).

2.2 Chemicals

The Pharmakon Collection (Microsource Discovery Systems) used in the chemical library screen contains 1600 FDA-approved drugs and is provided as 10 mM stocks in DMSO. Carbonyl cyanide 4-(trifluoromethoxy)- phenylhydrazone (FCCP) and purified compounds used in follow-up studies were purchased from Sigma Aldrich.

2.3 Oxygen consumption with biosensor plates

Trypsinized cells were resuspended in assay buffer (phenol-red free DMEM supplemented with 1 mM Na Pyruvate and 10% FBS), and cell concentration and viability were determined using a Vi-Cell counter (Beckman Coulter). Cells were aliquoted into 384-well oxygen Biosensor plates (BD Biosciences) and allowed to equilibrate for 20-30 min. DMSO or FCCP was added, and fluorescence was monitored using a Polar Star Omega plate reader (BMG Labtech, Germany) set at 37°C. For time traces, readings were taken every three minutes (485 nm excitation; 630 nm emission) for 90-120 min. For the endpoint assay, fluorescence was monitored at 0, 2 and 24 hours, and plates were incubated at 37 °C under 5% CO_2 between readings.

2.4 Chemical library screen

The library screen was carried out using the endpoint assay described above with the following specifications. 70,000 RGC-5 cells in 90 μL of assay buffer were aliquoted into each well of a 384-well Biosensor plate. Test compounds or vehicle were diluted in PBS then dispensed into wells without mixing, giving a final volume of 100 μL and final DMSO and test compound concentrations of 0.1% and 10 μM, respectively. Each plate contained 16 negative control (DMSO vehicle only) and 16 positive control (5 μM FCCP) wells. Test compounds were assayed in duplicate.

2.5 Oxygen consumption and proton production measurements using a Seahorse XF-24 system

For Bioenergetic profiling 50,000 FL83B mouse liver cells per well were seeded onto 24 well plates (Seahorse Biosciences, Billerica, MA) in 200 μl of DMEM-F12 media containing 10% FBS and 25 mM glucose and allowed to attach for 16 hours. For respiration analysis, media was changed to un-buffered cultured assay DMEM media containing 10% FBS, 22.5 mM mannitol, 1 mM Na Pyruvate, 2 mM Glutamax and 2.5 mM glucose at 37°C. Indicated concentrations of acarbose were added and cells were allowed to pre-equilibrate with fresh media and the drug for 1 hour at 37°C in a non-CO_2 incubator. The oxygen consumption rate (OCR) was measured using a Seahorse XF-24 instrument which is oxygen consumption per minute in pmols (pmols/min). Additionally, Extracellular Acidification

Rate (ECAR) was recorded and is a measure of glycolysis (Nicholls et al., 2010), the units are (mpH/min). Glucose was added after the first four cycles of OCR recording (baseline). Mannitol was used to smooth the osmotic differences as glucose concentration was increasing. Final concentrations in profile regimens were: Oligomycin: 1 μM, FCCP: 12.5 μM, Rotenone: 0.1 μM, Antimycin A: 1 μM, and glucose: 25 mM. Of note, optimal FCCP concentration was determined empirically in the presence of FBS in the running media.

265 Data analysis and statistics

Data are presented as Mean ± Standard Deviation (SD) or Mean ± Standard Error of the mean (SEM). The statistical significance of the screen data was determined with a two-tailed Student t test (p-value <0.05), and initial hits were scored as Vehicle Mean ± 2X Standard Deviation. Curve fits were performed using GraphPad prism nonlinear regression analysis with variable slope.

3. Results

3.1 Mitochondrial oxygen consumption can be measured in high throughput in normal and disease cell lines

BD Biosensor plates contain an oxygen-quenched probe that fluoresces as oxygen is removed from the plate well (Rolo et al., 2009; Wodnicka et al., 2000). In order to determine whether the 384-well version of the Biosensor plate is sufficiently sensitive to be useful in high-throughput screening, we measured FCCP-induced changes in oxygen consumption in a variety of cell lines (Fig. 1). In untreated cells, mitochondrial activity is regulated according to the energy needs of the cell. FCCP uncouples the mitochondrial electron transport chain from ATP synthesis, allowing the mitochondria to operate at maximum capacity (Brennan et al., 2006; Maro et al., 1982). As expected, cell lines with origins in tissues with high metabolic demands such as muscle or neuronal tissues showed large responses to FCCP. C2C12 mouse myoblasts (Blau et al., 1985; Katagiri et al., 1994; Yaffe and Saxel, 1977), 3T3 mammalian fibroblasts (Green and Kehinde, 1974; Jainchill et al., 1969), and 50B11 dorsal root ganglion (Chen et al., 2007) all responded strongly to FCCP. Lymphoblasts and leukemia cells, which typically have fewer mitochondria, showed a more modest response to FCCP.

Additionally, we evaluated cell models of LHON and FXTAS diseases in which mitochondrial functional defects have been demonstrated (Ross-Inta et al., 2010; Wallace et al., 1988). Basal and FCCP-stimulated oxygen consumption was measured in healthy and FXTAS cultured dermal fibroblasts (Fig 2a). Control and Leber's hereditary optic neuropathy osteosarcoma-derived cybrids (11778/ND4) were also evaluated (Fig 2b). We observed diminished oxygen consumption in the diseased cell lines compared to their non-diseased controls, with the larger difference uncovered by FCCP-stimulation. These functional changes in disease cell lines support the use of the assay as a platform to screen for therapeutics to rescue specific mitochondrial defects.

3.2 Optimization and conversion to endpoint format make the biosensor assay suitable for HTS

We next optimized the assay for high-throughput screening using retinal ganglion cells. In addition to using plates with the capacity to measure responses in 384-wells simultaneously, we carefully evaluated multiple assay parameters. These included selection of an optimal cell line, varying cell number, well volumes, temperature, and liquid handling methods. Perhaps most importantly was a decision to convert the method to an endpoint measurement, which allowed faster plate throughput and minimized variability of oxygen consumption rates. Together, these parameters increased signal to noise and minimized variability.

The RGC-5 cell line was chosen for the pilot screen because it is stable through many passages, grows well in culture, and forms uniform cell suspensions. Retinal ganglion cells are neurons that specifically degenerate in the mitochondrial disease LHON (Kwittken and Barest, 1958; Sadun et al., 1994). In the biosensor oxygen consumption assay, RGC-5 cells exhibited a robust signal-to-noise ratio and a dose-dependent increase in oxygen consumption in response to FCCP over 1.5 hours (Fig. 3). The required FCCP concentrations to reach maximal rates are likely influenced by serum presence in the assay (Jekabsons and Nicholls, 2006).

Although the kinetics were robust and the slopes clearly differed across a range of FCCP concentrations, there was some well-to-well variability among individual well traces, particularly for higher concentrations of FCCP at time points earlier than 60 minutes. For this reason, we converted to an endpoint assay, taking a single plate reading immediately after drug addition (t_0) and then again after 2- and 24-hour incubation periods. The fold change from baseline (FCB) was calculated by normalizing post-incubation readings to the t0 reading. This normalization helped to minimize effects due to well-to-well variation and eliminated potential false positives generated by compound fluorescence. FCB responses for drug-treated wells were then normalized to the average FCB for the 16 vehicle-treated wells producing the fold change from vehicle (FCV) value for each well. Conversion to an endpoint assay increased the average z’ to 0.8. Use of the endpoint assay also increased throughput by decreasing the amount of plate reader time required for each sample and by allowing us to stagger drug addition and plate reading sessions.

3.3 Screen of drug library identified activators and inhibitors of oxygen consumption

We used the biosensor endpoint assay to screen a library of 1600 drugs that have reached clinical evaluation in the United States. Drugs that increased or decreased oxygen consumption at vehicle mean plus or minus two standard deviations were considered significant “hits” and were assayed again. Retesting confirmed 19 activators and 17 inhibitors in the short term (2 hours), and 23 activators and 16 inhibitors in the long term (24 hours) (Fig. 4). Some drugs were active at both time points. The strongest activators and inhibitors at 2 and 24 hours are shown in Table 1.

3.4 The majority of confirmed hits demonstrate dose-dependent activity

Confirmed hits from the primary screen were then retested in the biosensor endpoint assay at concentrations ranging from 0.03-10 μM. Approximately 40% of the compounds identified

as activators and 70% of the compounds identified as inhibitors in both long and short-term experiments demonstrated dose dependent activity (Table 2). Representative concentration curves are shown in Figure 5. Dose-dependent increases in oxygen consumption were shown by many compounds, including acarbose at 2 hours (EC_{50}: 1.6±1.57 μM, n=3) (Fig. 5a); and enilconazole at 24 hours (EC_{50}: 0.46±1.4 μM, n=3) (Fig 5c). Dose-dependent mitochondrial inhibitors were also identified. For example, isoniazid significantly inhibited mitofunction at 2 hours (IC_{50}: 3.4±1.2 μM, n=3) (Fig 5b); and chlormadinone significantly inhibited at 24 hours (IC_{50}: 2.5±2.1 μM, n=3) (Fig 5d).

3.5 Acarbose's activity in biosensor plates is blocked by inhibitors of oxidative phosphorylation

Since acarbose is an anti-diabetic that is so widely used, we decided to explore this mitochondrial mechanistic interaction further. Though it has been suggested to interact with mitochondrial KATP channels (Minatoguchi et al., 2009), agonism of mitochondrial function by acarbose has not previously been recognized. If acarbose acts by increasing the flow of electrons through the mitochondrial respiratory chain, then this flow should be severely reduced by rotenone (complex I inhibitor) or oligomycin (ATP synthase inhibitor) (Ernster et al., 1963; Huijing and Slater, 1961). We used the endpoint assay in oxygen biosensor plates to monitor oxygen consumption in RGC-5 cells in the presence of acarbose and vehicle, rotenone or oligomycin. We found that acarbose's ability to increase oxygen consumption was blocked by either rotenone or oligomycin (Fig. 6a) (Ernster et al., 1963; Huijing and Slater, 1961).

Although the screen was performed in a cell line with healthy mitochondria, it seemed likely that some of the activators identified would be able to increase mitochondrial activity in a diseased cell line, particularly if the drug target functions downstream of the defect caused by the disease. In order to test whether acarbose could also increase mitochondrial activity in a diseased cell line, we treated control and LHON cybrids with acarbose and then measured their oxygen consumption in using the endpoint assay. Acarbose did not stimulate oxygen consumption in the LHON cybrids (Fig. 6b). However, because acarbose also has no effect on healthy cybrids, the lack of effect may be due to the cybrids' osteosarcoma cell background. Also, it should be noted that FCCP has a much weaker effect in cybrids than it does in RGC-5 cells, suggesting that the effect of a mild activator may not be detectable in cybrids.

3.6 Acarbose increases glucose-stimulated mitochondrial function using a Seahorse XF-24 system

To explore the acarbose effects on oxygen consumption further, we examined cellular bioenergetics using a Seahorse extracellular flux analyzer. We measured mitochondrial respiration and glycolysis simultaneously after acarbose treatment. 5L853B cells were chosen since they are an insulin-sensitive hepatic cell line (Breslow et al., 1973). Sample traces for oxygen consumption rate (OCR) in FL83B cells treated with 7.5 μM acarbose show clear increases in OCR after 25 mM glucose addition and 12.5 μM FCCP compared to vehicle (Fig. 7a). Acarbose is likely not an uncoupler, because after inhibition of mitochondrial complex V with oligomycin (Fig. 7a, rate section B), the OCR is the largely

the same in acarbose treated and vehicle treated cells. Oxygen consumption rates with inhibition of complex V is largely driven by mitochondrial proton leak and when cells treated with a mild uncoupler should have a higher OCR after the oligomycin regimen (David G et al., 2010). Also, as seen in the OCR increases between C and D (Fig 7a), acarbose seems to increase spare mitochondrial respiratory capacity. Analysis of OCR area under the curve after glucose stimulation shows clear dose-dependent increases following treatment with 2.5 – 10 μM acarbose (Fig. 7b). OCR normalized to Extracellular acidification rate (ECAR) in response to glucose was also increased with acarbose addition (Fig 7c). The OCR/ECAR ratio for vehicle and 7.5 μM acarbose treated cells was 11.8±2.13 versus 17.9±4.3 respectively (p=0.05, n=4).

We have shown acarbose effects on oxygen consumption in both oxygen biosensor plates and a Seahorse extracellular flux analyzer. Additionally using the Seahorse, we show an increased OCR/ECAR ratio, which indicates a shift to more active mitochondrial oxidation and reduced reliance of acarbose treated cells on glycolysis (David G et al., 2010). Taken together, while acarbose's effects on mitochondria may not be direct, it has a convincing effect on cellular energy metabolism that results in enhanced respiratory rates.

4. Discussion

4.1 Mitochondrial Oxygen consumption can be measured robustly in 384-well plates

The consumption of oxygen in the process of metabolite oxidation and ATP synthesis is the most commonly-used measure of mitochondrial function (Mandel, 1986). Using biosensor plates with a dye that fluoresces as Oxygen is consumed, we have established a robust, sensitive, and reproducible screening assay capable of identifying modulators of mitochondrial function in the short (2 hours) and long term (24 hours). In a 384-well format, our validated assay produces %CV values below 10% and an average z-prime value of 0.8, which indicates its usefulness in high-throughput systems and makes this assay an excellent platform for drug screening.

4.2 Mitochondrial activators identified in the screen are candidates for drug repurposing

Because mitochondrial diseases generally affect a small number of people, there are reduced incentives for the pharmaceutical industry to pursue treatments for these “orphan” indications. Thus, one strategy for mitochondrial disease therapy is to examine drugs that have already been approved for use in human patients for previously unrecognized effects on mitochondrial function with the hope that such drugs could be “repurposed” into a new therapeutic indication (Oprea and Mestres, 2012). This strategy would ideally shorten the development path since many of the safety and pharmacokinetic parameters of these drugs are already known. Our pilot screen in oxygen biosensor plates has identified mitochondrial stimulatory activity in a number of clinically evaluated compounds, indicating that the approach is valid, although we have not yet demonstrated rescue of a diseased cell line by any of our confirmed hits. Future drug screens for mito-functional rescue may need to be carried out in target cell lines bearing the relevant disease mutations.

4.3 The high throughput mitoassay identifies previously recognized mitochondrially active drugs

After screening the drug library and using the two-times the standard deviation (2xStDev) criterion of vehicle-treated wells, 17 compounds were found to be short term mitochondrial inhibitors (1.1%), 16 were long-term mitochondrial inhibitors (1%), and 15 were both short- and long-term inhibitors (0.9%), demonstrating high mitochondrial inhibitory overlap. About 70% of compounds identified as inhibitors in both long and short-term experiments repeated in concentration curves. Examples of mitochondrial inhibitors included decoquinate, isoniazid, suramin, erythrosine, toltrazuril, enilconazole, and metformin.

Decoquinate is a Coenzyme Q-like anti-coccidial agent that is known to interfere with mitochondrial electron transfer (Williams, 1997; Winter et al., 2008). Isoniazid is an anti-tuberculosis drug known to interact with mitochondria (Schwab and Tuschl, 2003). The chemotherapeutic suramin has been shown to inhibit oxygen consumption in intact mitochondria (Calcaterra et al., 1988). Erythrosine is a component of food colorings and has been reported to hinder mitochondrial ATPase function (Cocucci, 1986). Toltrazuril is an anticoccidial known to interact with mitochondrial pyrimidine biosynthesis linked to the respiratory chain, thus it presumably hits the mitochondrial dihydroorotate dehydrogenase target (Harder and Haberkorn, 1989; Jöckel et al., 1998). Enilconazole was previously shown to inhibit mitochondrial respiration (Nakagawa and Moore, 1995) and mitochondrial steroid biosynthesis (Drummond et al., 1988). Additionally, a previous study by Wagner et. al. tested a large and diverse chemical library on multiple cell-based assays of mitochondrial function, and identified statins to have inhibitory properties on the mitochondria (Wagner et al., 2008). However, statins were not a large chemical class of actives in our work, likely due to differences in parameters measured. Thus the biosensor screen correctly identifies drugs with published consequences on mitochondrial function.

4.4 Mild mitochondrial inhibitors are a potential therapeutic class

Metformin has been previously shown to be a mitochondrial complex I inhibitor (Owen et al., 2000). This anti-diabetic of the biguanide class lowers blood glucose by stimulating AMPK in the liver, causing an AMPK-dependent suppression of hepatic glucose export (Zhou et al., 2001). Thus, there can be a specific therapeutic benefit to the mild inhibition of mitochondrial function.

The main message from this study of inhibitors is that mild mitochondrial inhibition is not necessarily contraindicated in therapeutic drugs. In our study >1% of FDA-approved compounds have significant mitochondrial inhibitory activity, for some of them (metformin, decoquinate) the mild mitochondrial inhibitory activity of the drug *is* its known, therapeutic mechanism of action. For example, mild mitochondrial inhibition such as occurs by metformin through activation of AMPK, triggers a major shift in cellular metabolism that is therapeutic in the context of type II diabetes (Lage et al., 2008; Leclerc et al., 2004; Scott et al., 2004), and is being investigated in cancer (Buzzai et al., 2007; Evans et al., 2005; Scott et al., 2004).

4.5 The screening platform identifies novel mitofunctional activities of known drugs

There were several novel modulators of mitochondrial function identified. One of the most potent activators was Flumazenil. Flumazenil is used as a stimulant for patients who have been over-sedated and preferentially works through the central nervous system benzodiazepine receptor(Mukhin et al., 1989). Flumazenil interacts with the mitochondrial (peripheral) benzodiazepene receptor (Anholt et al., 1986; Price et al., 1993), has been shown to generate hydrogen peroxide, a known mitochondrial KATP channel opener (Yao et al., 2001; Zhang et al., 2002; Zhang and Yao, 2000). Metaraminol is an adrenergic alpha-1 agonist that functions as a vasoconstrictor, that is used in the prevention and treatment of hypotension, especially as a consequence of (over)-anesthesia (Kee et al., 2001; Lucas et al., 1966). The link between metaraminol and mitochondrial function is not known. However, alpha-adrenergic receptors stimulate IP3 and Ca^{2+} release, and calcium entry into the mitochondria results in an increase in oxidative-phosphorylation and ATP production (Brookes et al., 2004). Gallamine triethiodide is a M2 subtype muscarinic acetylcholine receptor antagonist used as a muscle relaxant (Goat et al., 1976; Leppik et al., 1994). M2 muscarinic receptors are G_i-coupled, and activation of these receptors would lead to a suppression of cAMP production and less Ca^{2+} release from the sarcoplasmic reticulum (Bugrim, 1999). Thus gallamine-mediated inhibition of this pathway would lead to increased calcium release and potential mitochondrial uptake of calcium (McCormack and Denton, 1993). However, in parallel to these studies on mitochondrial function, we measured tubulin protein expression and DNA quantity using CyQuant in cells after treatment with all 1600 drugs. Galalmine was one of the very few oxygen consumption modulators that also inhibited tubulin by ~20% (*not shown*). Thus, it is possible this inhibition is due to toxicity. Acamprosate is a NMDA receptor modulator used to suppress cravings (Naassila et al., 1998). Acamprosate has been shown to inhibit microsomal Ca^{2+-} ATPase and leads to an increase in reactive oxygen species, which could affect mitochondrial function (Çalışkan et al., 2010). All three of these drugs (metaraminol, gallamine, acamprosate) inhibited mitochondrial oxygen consumption in RGC-5 cells (Table 1), representing potential novel additional mechanisms of action involving the mitochondria for these compounds.

Acarbose is an anti-diabetic oligosaccharide whose canonical mechanism is through inhibition of glucosidase activity in the intestine. The delay of polysaccharide digestion in the intestine is thought to lower carbohydrate uptake and glucose absorption (Balfour and McTavish, 1993; Matthaei et al., 2000). Though acarbose is absorbed into the blood (~2%), its therapeutic effects are thought to take place before entry into the central compartment (Ahr et al., 1989). We find that acarbose strongly induces mitochondrial function in cells (Fig. 5a), and that this induction is cancelled by the specific mitochondrial electron transport chain inhibitors (Fig 6a). Furthermore, bioenergetic profiling of FL83B cells revealed increasing OCR with increasing acarbose doses (Fig. 7b), suggesting that it specifically activates mitochondrial respiration. Additionally, we have shown acarbose increased phospho-AMPK protein in FL83B cells (*data not shown*). Thus an additional therapeutic mechanism not previously described for acarbose is the activation of mitochondrial activity, perhaps through AMPK activation. This could support increased lipid oxidation and and reduced glycolysis. Acarbose has been shown to lower inflammatory and oxidative stress related to low-density lipoprotein in post-meal diabetic models *in vivo* (Derosa et al., 2011;

Inoue et al., 2006). However, direct mitochondrial effects of acarbose have not been previously described.

Here we have described an improved assay with the ability to detect modulators of mitochondrial function in high throughput. The assay identifies known mitochondrial modulators (e.g metformin, decoquinate), and previously unknown mitochondrial modulators (e.g. acarbose, metaraminol). It is possible that these previously unrecognized impacts on mitofunction could be downstream of the primary drug target. Alternatively, they could be secondary 'off target' effects in the sense that the drug hits a second target that regulates mitofunction. The work shows that there are clearly FDA- approved drugs with previously unrecognized mitochondrial effects, highlighting the importance of mitochondrial function in pharmacology and toxicology (Scatena et al., 2007). Compounds identified to “accidentally” interact with the mitochondria have been reviewed, and include diverse therapeutic and mechanistic classes such as potassium channel openers, anti-diabetics, anti-cancer, anti-viral, nonsteroidal anti-inflammatory and local anesthetic compounds (Szewczyk and Wojtczak, 2002). Since the mitochondria plays a diverse role in cellular homeostasis and signaling, it is not surprising that it is a frequent pharmacological target. Discovering unwanted secondary effects of compounds in drug development is paramount to drug safety (Dykens and Will, 2007; Scatena et al., 2007; Szewczyk and Wojtczak, 2002). Thus, determining secondary mitochondrial effects of compounds could help make medicines safer, and this high-throughput assay platform of mitochondrial function can possibly aid in the identification process.

5. Conclusions

We have demonstrated that a robust assay of mitochondrial function is possible in 384-well format, with low variability. The platform discriminates mitofunctional differences in LHON and FXTAS cell models. The assay was used to screen 1600 drugs that have been clinically evaluated. Multiple drugs known to inhibit mitochondrial function such as metformin and decoquinate were confirmed to inhibit mitochondrial oxygen consumption in RGC-5 cells. Additionally, several drugs with no previously-known mitofunctional effects were identified, including acarbose, metaraminol, gallamine triethiodide, and acamprosate. Our hope is that the identification of these mitochondrially active drugs could represent potential new leads to treat orphan mitochondrial diseases.

Acknowledgments

This work was supported by awards from the NIH: RO1 NS077777, RO1 EY012245, PO1 AG025532; the MDA 157798, and ARO to GAC, and the NICHD HD40661 to PJH

Abbreviations

FXTAS	Fragile X Syndrome
LHON	Leber's Hereditary Neuropathy
AMPK	AMP-activated protein kinase

OCR	oxygen consumption rate
ECAR	extracellular acidification rate

References

Ahr H, Boberg M, Krause H, Maul W, Müller F, Ploschke H, Weber H, Wünsche C. Pharmacokinetics of acarbose. Part I: Absorption, concentration in plasma, metabolism and excretion after single administration of [14C] acarbose to rats, dogs and man. Arzneimittel-Forschung. 1989; 39:1254–1260. [PubMed: 2610717]

Anholt R, Pedersen P, De Souza E, Snyder S. The peripheral-type benzodiazepine receptor. Localization to the mitochondrial outer membrane. Journal of Biological Chemistry. 1986; 261:576–583. [PubMed: 3001071]

Armstrong J. Mitochondrial medicine: pharmacological targeting of mitochondria in disease. British journal of pharmacology. 2007; 151:1154–1165. [PubMed: 17519949]

Balfour JA, McTavish D. Acarbose. Drugs. 1993; 46:1025–1054. [PubMed: 7510610]

Blau HM, Pavlath GK, Hardeman EC, Chiu C-P, Silberstein L, Webster SG, Miller SC, Webster C. Plasticity of the differentiated state. Science. 1985; 230:758–766. [PubMed: 2414846]

Brennan JP, Southworth R, Medina RA, Davidson SM, Duchen MR, Shattock MJ. Mitochondrial uncoupling, with low concentration FCCP, induces ROS-dependent cardioprotection independent of KATP channel activation. Cardiovascular research. 2006; 72:313–321. [PubMed: 16950237]

Breslow J, Sloan H, Ferrans V, Anderson J, Levy R. Characterization of the mouse liver cell line FL83B. Experimental cell research. 1973; 78:441–453. [PubMed: 4572697]

Brookes PS, Yoon Y, Robotham JL, Anders M, Sheu S-S. Calcium, ATP, and ROS: a mitochondrial love-hate triangle. American Journal of Physiology-Cell Physiology. 2004; 287:C817–C833. [PubMed: 15355853]

Bugrim A. Regulation of Ca< sup> 2+</sup> release by cAMP-dependent protein kinase A mechanism for agonist-specific calcium signaling? Cell calcium. 1999; 25:219–226. [PubMed: 10378083]

Buzzai M, Jones RG, Amaravadi RK, Lum JJ, DeBerardinis RJ, Zhao F, Viollet B, Thompson CB. Systemic treatment with the antidiabetic drug metformin selectively impairs p53-deficient tumor cell growth. Cancer research. 2007; 67:6745–6752. [PubMed: 17638885]

Calcaterra NB, Vicario LR, Roveri OA. Inhibition by suramin of mitochondrial ATP synthesis. Biochemical pharmacology. 1988; 37:2521–2527. [PubMed: 2968800]

Çalışkan AM, Nazıroğlu M, Uğuz AC, Övey İS, Sütçü R, Bal R, Çalışkan S, Özcankaya R. Acamprosate modulates alcohol-induced hippocampal NMDA receptors and brain microsomal Ca2+-ATPase but induces oxidative stress in rat. The Journal of membrane biology. 2010; 237:51–58. [PubMed: 20871985]

Chen W, Mi R, Haughey N, Oz M, Höke A. Immortalization and characterization of a nociceptive dorsal root ganglion sensory neuronal line. Journal of the Peripheral Nervous System. 2007; 12:121–130. [PubMed: 17565537]

Cocucci MC. Inhibition of plasma membrane and tonoplast ATPases by erythrosin B. Plant science. 1986; 47:21–27.

David G,N, Victor M,D-U, Min W, Per Bo, J. George W,R. Bioenergetic profile experiment using C2C12 myoblast cells. Journal of Visualized Experiments. 2010

Derosa G, Maffioli P, Ferrari I, Fogari E, D'Angelo A, Palumbo I, Randazzo S, Bianchi L, Cicero AF. Acarbose actions on insulin resistance and inflammatory parameters during an oral fat load. European journal of pharmacology. 2011; 651:240–250. [PubMed: 21118681]

Drummond TD, Ian Mason J, McCarthy JL. Gerbil adrenal 11β-and 19-hydroxylating activities respond similarly to inhibitory or stimulatory agents: two activities of a single enzyme. Journal of steroid biochemistry. 1988; 29:641–648. [PubMed: 3386231]

Dykens JA, Will Y. The significance of mitochondrial toxicity testing in drug development. Drug discovery today. 2007; 12:777–785. [PubMed: 17826691]

Ernster L, Dallner G, Azzone GF. Differential effects of rotenone and amytal on mitochondrial electron and energy transfer. Journal of Biological Chemistry. 1963; 238:1124–1131.

Evans JM, Donnelly LA, Emslie-Smith AM, Alessi DR, Morris AD. Metformin and reduced risk of cancer in diabetic patients. Bmj. 2005; 330:1304–1305. [PubMed: 15849206]

Goat V, Yeung M, Blakeney C, Feldman S. The effect of blood flow upon the activity of gallamine triethiodide. British journal of anaesthesia. 1976; 48:69–74. [PubMed: 1252317]

Goto, Y.-i.; Horai, S.; Matsuoka, T.; Koga, Y.; Nihei, K.; Kobayashi, M.; Nonaka, I. Mitochondrial myopathy, encephalopathy, lactic acidosis, and stroke-like episodes (MELAS) A correlative study of the clinical features and mitochondrial DNA mutation. Neurology. 1992; 42:545–545. [PubMed: 1549215]

Green H, Kehinde O. Sublines of mouse 3T3 cells that accumulate lipid. Cell. 1974; 1:113–116.

Harder A, Haberkorn A. Possible mode of action of toltrazuril: studies on twoEimeria species and mammalian andAscaris suum enzymes. Parasitology research. 1989; 76:8–12. [PubMed: 2560189]

Hirai K, Aliev G, Nunomura A, Fujioka H, Russell RL, Atwood CS, Johnson AB, Kress Y, Vinters HV, Tabaton M. Mitochondrial abnormalities in Alzheimer's disease. The Journal of Neuroscience. 2001; 21:3017–3023. [PubMed: 11312286]

Huijing F, Slater E. The use of oligomycin as an inhibitor of oxidative phosphorylation. Journal of biochemistry. 1961; 49:493–501. [PubMed: 13716716]

Inoue I, Shinoda Y, Nakano T, Sassa M, Goto S.-i. Awata T, Komoda T, Katayama S. Acarbose ameliorates atherogenecity of low-density lipoprotein in patients with impaired glucose tolerance. Metabolism. 2006; 55:946–952. [PubMed: 16784969]

Jainchill JL, Aaronson SA, Todaro GJ. Murine sarcoma and leukemia viruses: assay using clonal lines of contact-inhibited mouse cells. Journal of Virology. 1969; 4:549–553. [PubMed: 4311790]

Jekabsons M, Nicholls D. Bioenergetic analysis of cerebellar granule neurons undergoing apoptosis by potassium/serum deprivation. Cell Death & Differentiation. 2006; 13:1595–1610. [PubMed: 16410795]

Jöckel J, Wendt B, Löffler M. Structural and functional comparison of agents interfering with dihydroorotate, succinate and NADH oxidation of rat liver mitochondria. Biochemical pharmacology. 1998; 56:1053–1060. [PubMed: 9776318]

Kaplan J. Friedreich's ataxia is a mitochondrial disorder. Proceedings of the National Academy of Sciences. 1999; 96:10948–10949.

Katagiri T, Yamaguchi A, Komaki M, Abe E, Takahashi N, Ikeda T, Rosen V, Wozney JM, Fujisawa-Sehara A, Suda T. Bone morphogenetic protein-2 converts the differentiation pathway of C2C12 myoblasts into the osteoblast lineage. The Journal of cell biology. 1994; 127:1755–1766. [PubMed: 7798324]

Kee WDN, Lau TK, Khaw KS, Lee BB. Comparison of metaraminol and ephedrine infusions for maintaining arterial pressure during spinal anesthesia for elective cesarean section. Anesthesiology. 2001; 95:307–313. [PubMed: 11506099]

Kwittken J, Barest HD. The neuropathology of hereditary optic atrophy (Leber's disease): the first complete anatomic study. The American journal of pathology. 1958; 34:185. [PubMed: 13498139]

Lage R, Diéguez C, Vidal-Puig A, López M. AMPK: a metabolic gauge regulating whole-body energy homeostasis. Trends in molecular medicine. 2008; 14:539–549. [PubMed: 18977694]

Leclerc I, Woltersdorf WW, da Silva Xavier G, Rowe RL, Cross SE, Korbutt GS, Rajotte RV, Smith R, Rutter GA. Metformin, but not leptin, regulates AMP-activated protein kinase in pancreatic islets: impact on glucose-stimulated insulin secretion. American Journal of Physiology-Endocrinology and Metabolism. 2004; 286:E1023–E1031. [PubMed: 14871885]

Leppik RA, Miller RC, Eck M, Paquet J-L. Role of acidic amino acids in the allosteric modulation by gallamine of antagonist binding at the m2 muscarinic acetylcholine receptor. Molecular pharmacology. 1994; 45:983–990. [PubMed: 8190113]

Lucas W, Kirschbaum T, Assali N, Beck R, Paler J. Effects of Autonomic Blockade with Spinal Anesthesia on Uterine and Fetal Hemodynamies and Oxygen Consumption in the Sheep. Neonatology. 1966; 10:166–179.

Mandel L. Primary active sodium transport, oxygen consumption, and ATP: coupling and regulation. Kidney international. 1986; 29:3. [PubMed: 3007851]

Maro B, Marty M-C, Bornens M. In vivo and in vitro effects of the mitochondrial uncoupler FCCP on microtubules. The EMBO journal. 1982; 1:1347. [PubMed: 6765194]

Matthaei S, Stumvoll M, Kellerer M, Haring H-U. Pathophysiology and Pharmacological Treatment of Insulin Resistance 1. Endocrine reviews. 2000; 21:585–618. [PubMed: 11133066]

McCormack J, Denton R. Mitochondrial Ca2+ transport and the role of intramitochondrial Ca2+ in the regulation of energy metabolism. Developmental neuroscience. 1993; 15:165–173. [PubMed: 7805568]

Minatoguchi S, Zhang Z, Bao N, Kobayashi H, Yasuda S, Iwasa M, Sumi S, Kawamura I, Yamada Y, Nishigaki K. Acarbose reduces myocardial infarct size by preventing postprandial hyperglycemia and hydroxyl radical production and opening mitochondrial KATP channels in rabbits. Journal of cardiovascular pharmacology. 2009; 54:25–30. [PubMed: 19487955]

Mukhin AG, Papadopoulos V, Costa E, Krueger KE. Mitochondrial benzodiazepine receptors regulate steroid biosynthesis. Proceedings of the National Academy of Sciences. 1989; 86:9813–9816.

Naassila M, Hammoumi S, Legrand E, Durbin P, Daoust M. Mechanism of Action of Acamprosate. Part I. Characterization of Spermidine-Sensitive Acamprosate Binding Site in Rat Brain. Alcoholism: Clinical and Experimental Research. 1998; 22:802–809.

Nakagawa Y, Moore GA. Cytotoxic effects of postharvest fungicides, ortho-phenylphenol, thiabendazole and imazalil, on isolated rat hepatocytes. Life sciences. 1995; 57:1433–1440. [PubMed: 7674834]

Nicholls DG, Darley-Usmar VM, Wu M, Jensen PB, Rogers GW, Ferrick DA. Bioenergetic profile experiment using C2C12 myoblast cells. Journal of visualized experiments : JoVE. 2010

Oprea T, Mestres J. Drug repurposing: far beyond new targets for old drugs. The AAPS Journal. 2012; 14:759–763. [PubMed: 22826034]

Owen M, DORAN E, Halestrap A. Evidence that metformin exerts its anti-diabetic effects through inhibition of complex 1 of the mitochondrial respiratory chain. Biochem. J. 2000; 348:607–614. [PubMed: 10839993]

Price JC, Mayberg HS, Dannals RF, Wilson AA, Ravert HT, Sadzot B, Rattner Z, Kimball A, Feldman MA, Frost JJ. Measurement of benzodiazepine receptor number and affinity in humans using tracer kinetic modeling, positron emission tomography, and [11C] flumazenil. Journal of Cerebral Blood Flow & Metabolism. 1993; 13:656–667. [PubMed: 8391018]

Rolo AP, Palmeira CM, Cortopassi GA. Biosensor plates detect mitochondrial physiological regulators and mutations in vivo. Analytical biochemistry. 2009; 385:176–178. [PubMed: 18950600]

Ross-Inta C, Omanska-Klusek A, Wong S, Barrow C, Garcia-Arocena D, Iwahashi C, Berry-Kravis E, Hagerman R, Hagerman P, Giulivi C. Evidence of mitochondrial dysfunction in fragile X-associated tremor/ataxia syndrome. Biochem. J. 2010; 429:545–552. [PubMed: 20513237]

Sadun A, Kashima Y, Wurdeman A, Dao J, Heller K, Sherman J. MORPHOLOGICAL FINDINGS IN THE VISUAL-SYSTEM IN A CASE OF LEBERS HEREDITARY OPTIC NEUROPATHY. Clinical Neuroscience. 1994; 2:165–172.

Santorelli FM, Shanske S, Macaya A, DeVivo DC, DiMauro S. The mutation at nt 8993 of mitochondrial DNA is a common cause of Leigh's syndrome. Annals of neurology. 1993; 34:827–834. [PubMed: 8250532]

Scatena R, Bottoni P, Botta G, Martorana GE, Giardina B. The role of mitochondria in pharmacotoxicology: a reevaluation of an old, newly emerging topic. American Journal of Physiology-Cell Physiology. 2007; 293:C12–C21. [PubMed: 17475665]

Schapira A, Cooper J, Dexter D, Clark J, Jenner P, Marsden C. Mitochondrial complex I deficiency in Parkinson's disease. Journal of neurochemistry. 1990; 54:823–827. [PubMed: 2154550]

Schwab CE, Tuschl H. In vitro studies on the toxicity of isoniazid in different cell lines. Human & experimental toxicology. 2003; 22:607–615. [PubMed: 14686483]

Scott JW, Hawley SA, Green KA, Anis M, Stewart G, Scullion GA, Norman DG, Hardie DG. CBS domains form energy-sensing modules whose binding of adenosine ligands is disrupted by disease mutations. Journal of Clinical Investigation. 2004; 113:274–284. [PubMed: 14722619]

Shoffner JM, Lott MT, Lezza A, Seibel P, Ballinger SW, Wallace DC. Myoclonic epilepsy and ragged-red fiber disease (MERRF) is associated with a mitochondrial DNA tRNA< sup> Lys</ sup> mutation. Cell. 1990; 61:931–937. [PubMed: 2112427]

Szewczyk A, Wojtczak L. Mitochondria as a pharmacological target. Pharmacological reviews. 2002; 54:101–127. [PubMed: 11870261]

Toogood PL. Mitochondrial drugs. Current opinion in chemical biology. 2008; 12:457–463. [PubMed: 18602018]

Wagner BK, Kitami T, Gilbert TJ, Peck D, Ramanathan A, Schreiber SL, Golub TR, Mootha VK. Large-scale chemical dissection of mitochondrial function. Nature biotechnology. 2008; 26:343–351.

Wallace DC. Mitochondrial diseases in man and mouse. Science. 1999; 283:1482–1488. [PubMed: 10066162]

Wallace DC, Singh G, Lott MT, Hodge JA, Schurr TG, Lezza A, Elsas LJ, Nikoskelainen EK. Mitochondrial DNA mutation associated with Leber's hereditary optic neuropathy. Science. 1988; 242:1427–1430. [PubMed: 3201231]

Williams R. The mode of action of anticoccidial quinolones (6-decyloxy-4-hydroxyquinoline-3-carboxylates) in chickens. International journal for parasitology. 1997; 27:101–111. [PubMed: 9076535]

Winter RW, Kelly JX, Smilkstein MJ, Dodean R, Hinrichs D, Riscoe MK. Antimalarial quinolones: synthesis, potency, and mechanistic studies. Experimental parasitology. 2008; 118:487–497. [PubMed: 18082162]

Wodnicka M, Guarino RD, Hemperly JJ, Timmins MR, Stitt D, Pitner JB. Novel fluorescent technology platform for high throughput cytotoxicity and proliferation assays. Journal of biomolecular screening. 2000; 5:141–152. [PubMed: 10894757]

Wong PC, Pardo CA, Borchelt DR, Lee MK, Copeland NG, Jenkins NA, Sisodia SS, Cleveland DW, Price DL. An adverse property of a familial ALS-linked SOD1 mutation causes motor neuron disease characterized by vacuolar degeneration of mitochondria. Neuron. 1995; 14:1105–1116. [PubMed: 7605627]

Yaffe D, Saxel O. Serial passaging and differentiation of myogenic cells isolated from dystrophic mouse muscle. Nature. 1977; 270:725–727. [PubMed: 563524]

Yao Z, McPherson BC, Liu H, Shao Z, Li C, Qin Y, Hoek TLV, Becker LB, Schumacker PT. Signal transduction of flumazenil-induced preconditioning in myocytes. American Journal of Physiology-Heart and Circulatory Physiology. 2001; 280:H1249–H1255. [PubMed: 11179070]

Zhang HY, McPherson BC, Liu H, Baman TS, Rock P, Yao Z. H2O2 opens mitochondrial KATPchannels and inhibits GABA receptors via protein kinase C-ε in cardiomyocytes. American Journal of Physiology-Heart and Circulatory Physiology. 2002; 282:H1395–H1403. [PubMed: 11893576]

Zhang Q, Yao Z. Flumazenil preconditions cardiomyocytes via oxygen radicals and KATP channels. American Journal of Physiology-Heart and Circulatory Physiology. 2000; 279:H1858–H1863. [PubMed: 11009473]

Zhou G, Myers R, Li Y, Chen Y, Shen X, Fenyk-Melody J, Wu M, Ventre J, Doebber T, Fujii N. Role of AMP-activated protein kinase in mechanism of metformin action. Journal of Clinical Investigation. 2001; 108:1167–1174. [PubMed: 11602624]

Highlights

- 1600-FDA approved drugs are tested for effects on mitochondrial function
- Known mitomodulators were identified by the assay (metformin, decoquinate)
- Novel FDA-approved drugs not previously known to have mitofunctional effects were also identified, that could be considered for rescue of mitochondrial disease

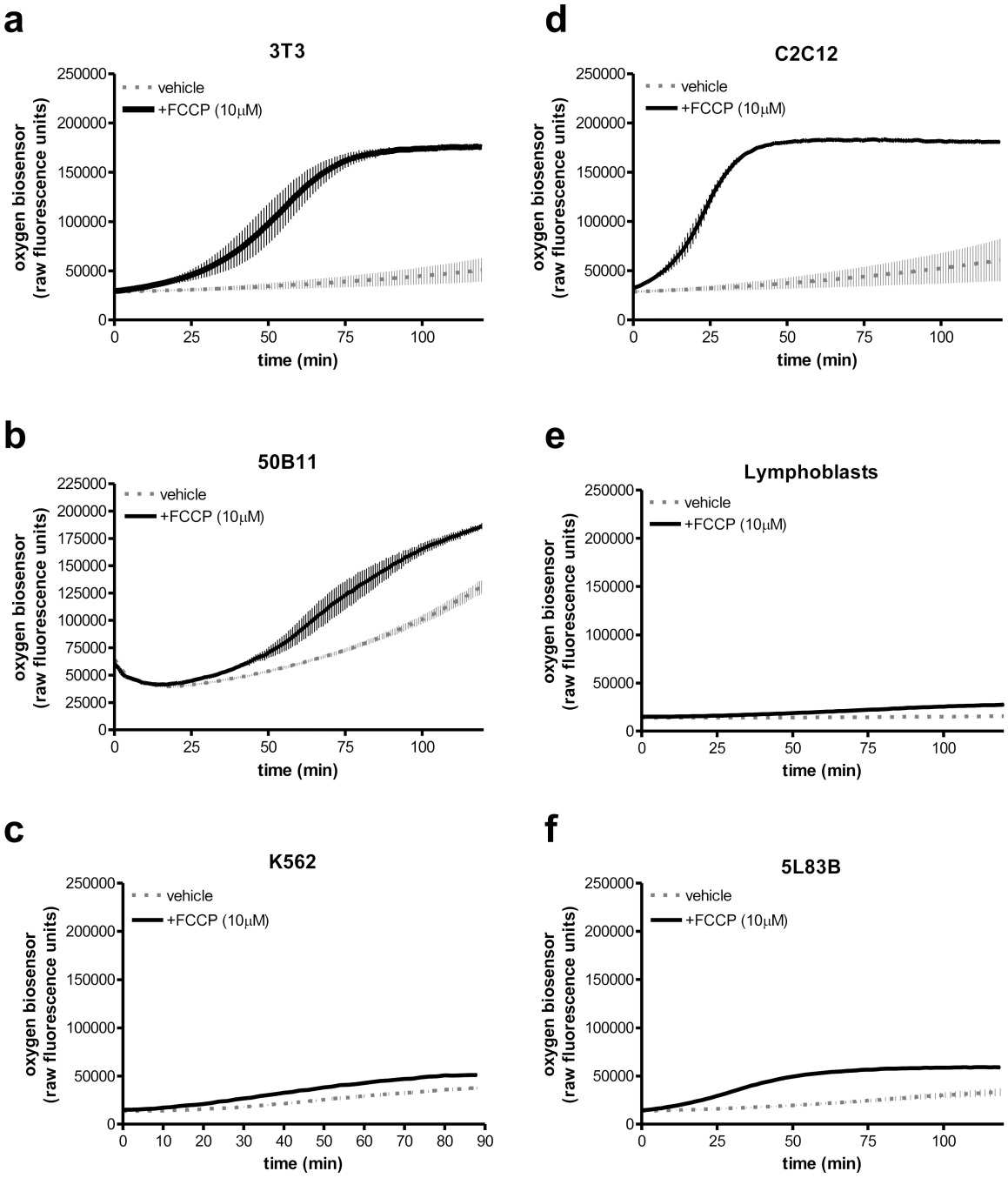

Figure 1.

Representative traces for oxygen consumption in (**a**) 3T3, (**b**) 50B11, (**c**) K562, (**d**) C2C12, (**e**) lymphoblasts, and (**f**) FL83B cells. Cells were aliquoted into 384-well Biosensor plates, and at t_0, either vehicle (grey traces) or 10 μM FCCP (black traces) was added. Fluorescence was monitored for 90-120 min. The plotted data displays mean reference fluorescence units (RFU), which correlate positively with oxygen consumption. Error bars represent SEM (*n* = *3*).

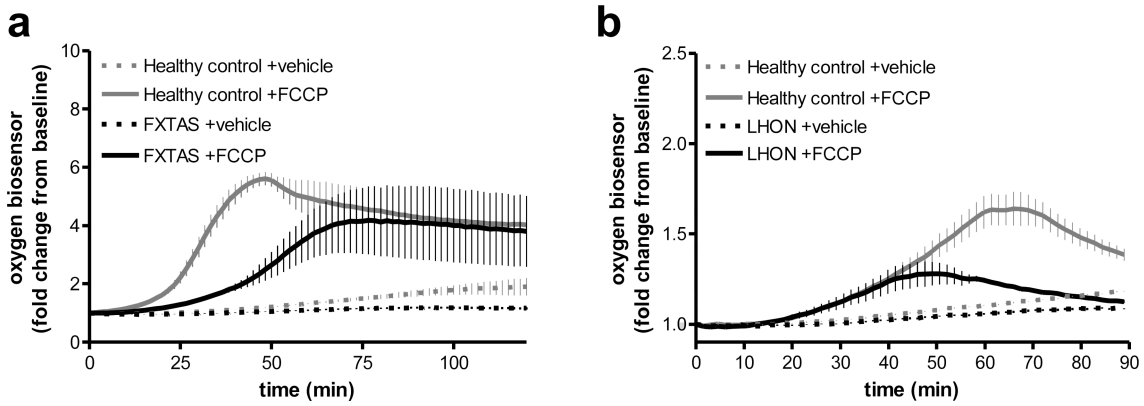

Figure 2.

Representative traces for oxygen consumption comparing (a) FXTAS fibroblasts to healthy fibroblasts or (b) LHON mutation 11778 cybrids to healthy cybrids. Cells were aliquoted into 384-well biosensor plates with either vehicle (dotted traces) or 10 μM FCCP (solid traces), and fluorescence was monitored for 90-120 min (n=4 wells). The plotted data displays mean fold change from baseline fluorescence at t_0. Error bars represent SEM (*n = 4*). We observed diminished oxygen consumption in the diseased cells (black traces) compared to healthy controls (grey traces) under both basal and FCCP-uncoupled conditions.

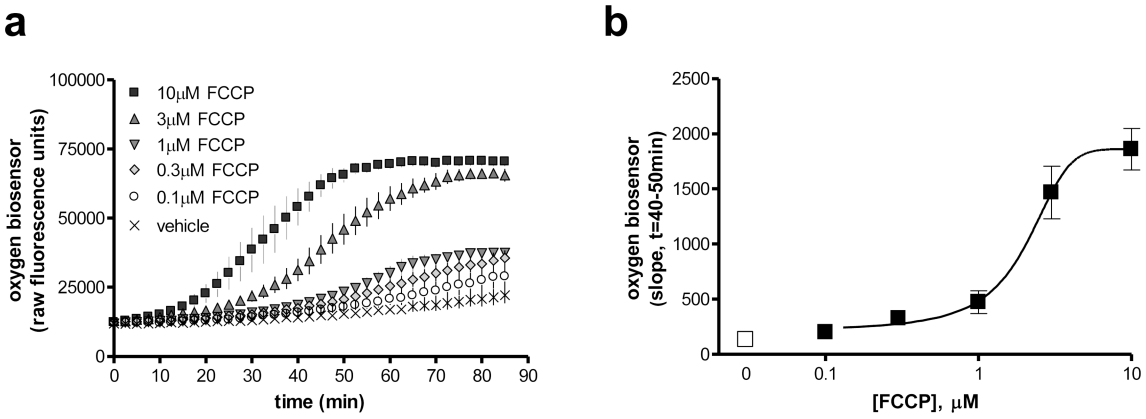

Figure 3.

FCCP stimulation of oxygen consumption in RGC-5 cells. (**a**) RGC-5 cells were aliquoted into 384-well biosensor plates with vehicle or FCCP at concentrations ranging from 0.1-10 μM. Fluorescence was monitored for 90 min (*n=4*). The plotted data displays mean reference fluorescence units (RFU), which correlate positively with oxygen consumption. (**b**) The mean slope of the curve in (a) from t=40-50 min is plotted as a function of FCCP concentration. Error bars represent SEM (*n = 4*).

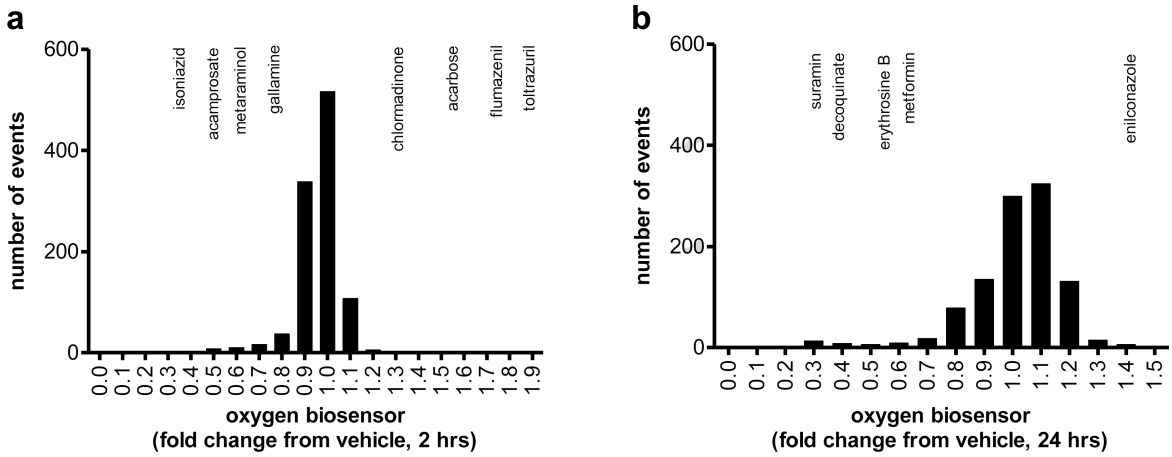

Figure 4.

Histograms of modulators of oxygen consumption identified by high-throughput drug screen in biosensor plates. The oxygen consumption biosensor assay was used to screen a library of 1600 drugs at 10 μM test concentration with endpoint readings at (**a**) 2 hours and (**b**) 24 hours. The vehicle control was 0.1% DMSO; the positive control was 5 μM FCCP. X-axes display mean fold change from vehicle (FCV) fluorescence at respective time points in bins of size 0.1 (duplicate). Mean FCCP response at 2 hours was 3.2 FCV. At 2 hours, the mean FCV for all drugs was 0.95 ± 0.107 SD. At 24 hours, the mean FCV for all drugs was 1.01 ± 0.16 SD. Drugs that increased or decreased oxygen consumption at vehicle mean ± two standard deviations were considered significant “hits”. Selected compounds are shown above bins corresponding to the FCV response for the drug.

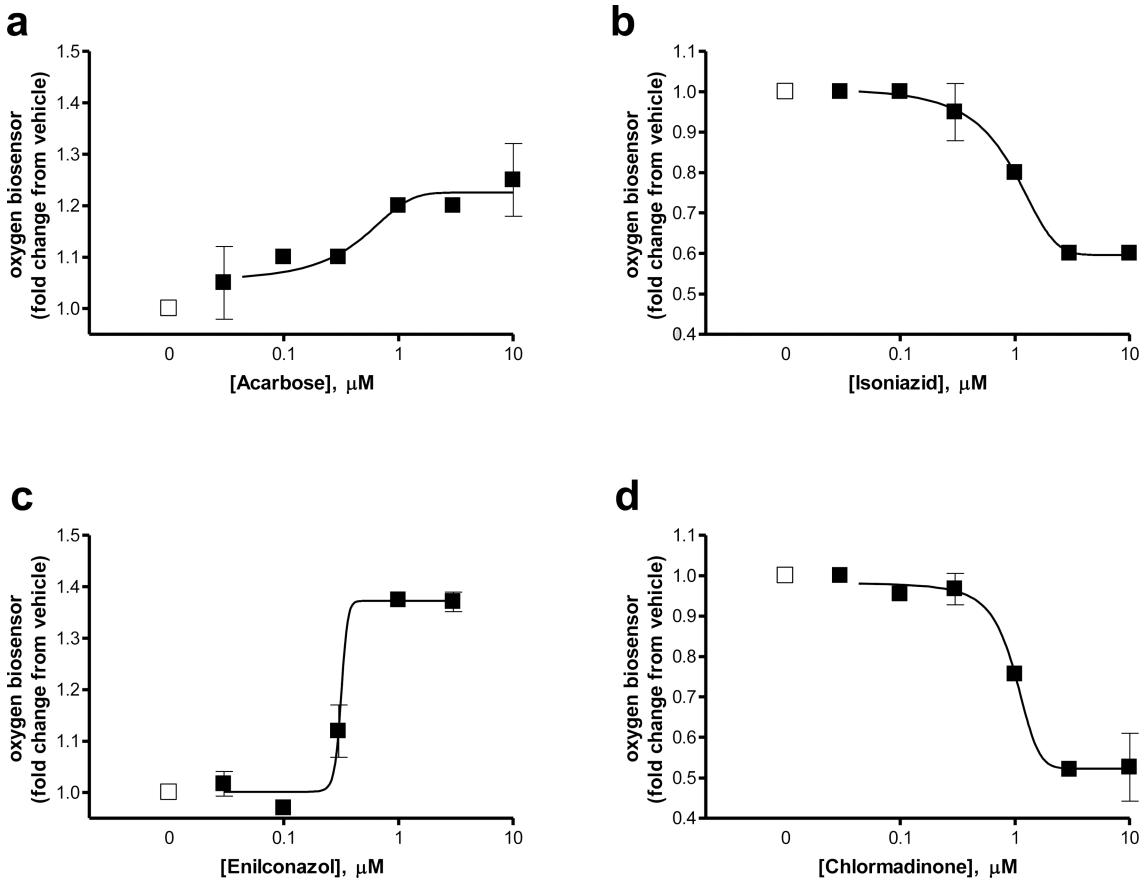

Figure 5.

Representative dose-response curves of short and long term oxygen consumption modulators in RGC-5 cells using oxygen biosensor plates. Compounds that reproducibly increased or decreased oxygen consumption at vehicle mean ± two standard deviations were tested using the endpoint assay in biosensor plates at additional concentrations ranging from 0.01–10 μM. The plotted data displays mean fold change from vehicle fluorescence at 2 or 24 hours. Error bars represent SEM (n = 3). Examples of dose dependent increases in oxygen consumption are shown for (**a**) acarbose at 2 hours (EC_{50}: 1.6±1.57 μM, n=3) and (**c**) enilconazole at 24 hours (EC_{50}: 0.46±1.4 μM, n=3). Examples of dose dependent decreases in oxygen consumption are shown for (**b**) isoniazid at 2 hours (IC_{50}: 3.4±1.2 μM, n=3) and (**d**) chlormadinone at 24 hours (IC_{50}: 2.5±2.1 μM, n=3).

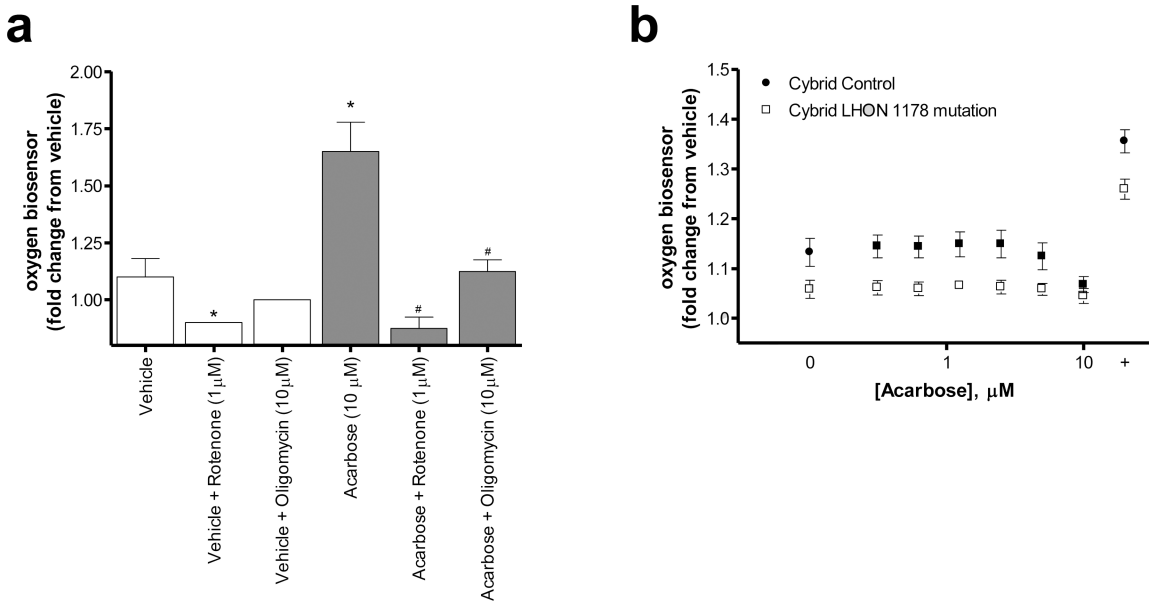

Figure 6.

Effect of mitochondrial toxins on acarbose activity. **(a)**RGC-5 cells were treated with vehicle (0.1% DMSO) or acarbose (10 μM), in combination with either the electron transport chain inhibitor rotenone (10 μM) or the ATP synthase inhibitor oligomycin (10 μM). All treatments were added at t_0, and oxygen consumption was measured at 2 hours using the endpoint assay. The plotted data displays mean fold change from vehicle fluorescence at 2 hours. Error bars represent SD (n = 4). $^{*}P < 0.05$, relative to vehicle control, t test. $^{\#}P < 0.05$, relative to vehicle control, t test. (**b**) Acarbose does not increase oxygen consumption in control or LHON 1178-mutation containing cybrid cells. Positive control is 5uM FCCP (+); Negative control is 0.1% DMSO (0). The plotted data displays mean fold change from vehicle fluorescence at 2 hours. Error bars represent SEM (n = 4).

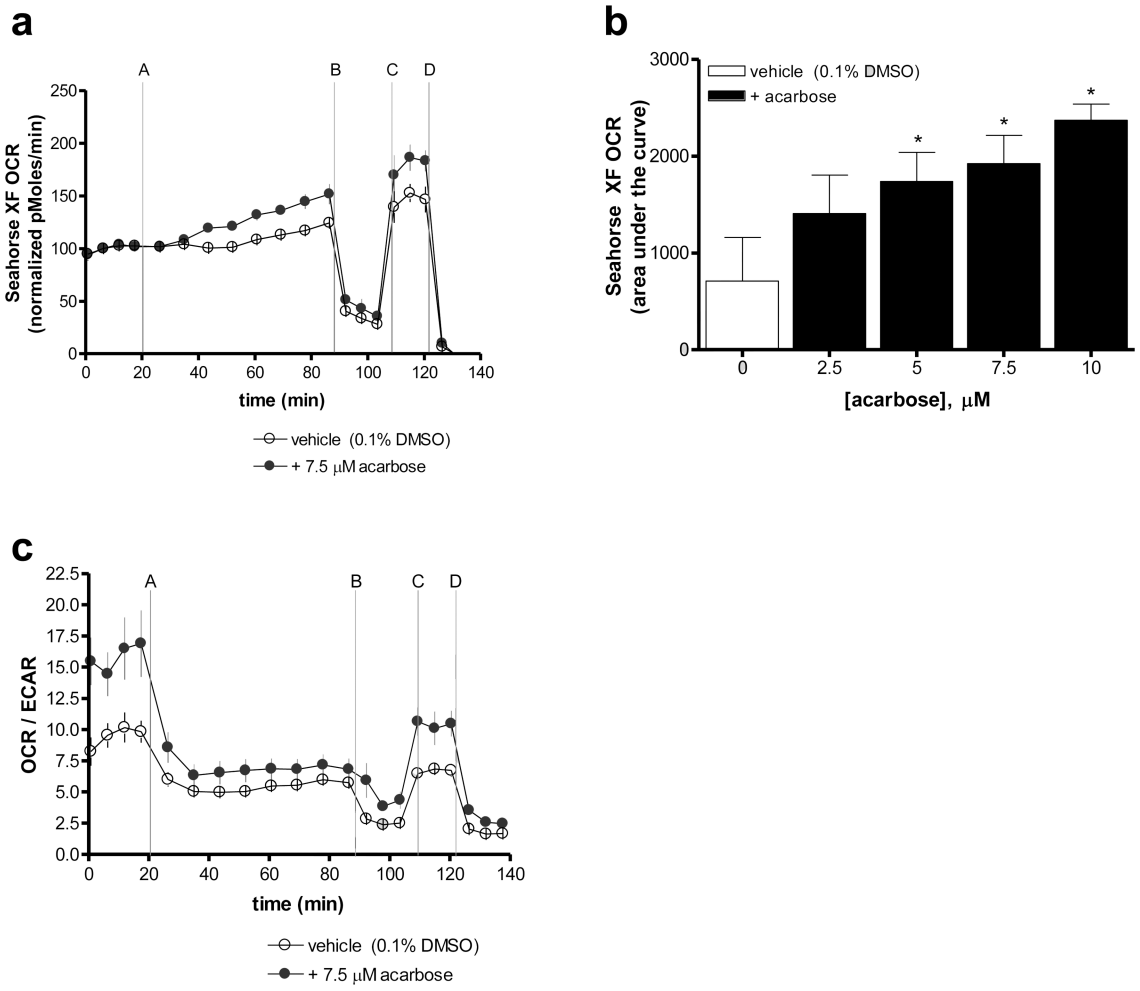

Figure 7.

Acarbose effects on cellular bioenergetics in FL83B cells. Seahorse extracellular flux analyzer allows measurement of mitochondrial respiration after acarbose treatment in 5L83B cells. (**a**) Representative traces for oxygen consumption rate (OCR) in FL83B cells pre-treated with 7.5 μM acarbose for one hour (A: 25 mM glucose, B: 1 μM oligomycin, C: 12.5 μM FCCP, D: 0.1 μM rotenone and 1 μM antimycin A). (**b**) Analysis of OCR area under the curve for 2.5 – 10 μM acarbose treated cells is shown. (**c**) Representative traces for ratio between OCR and extracellular acidification rate (ECAR) for FL83B cells pre-treated with 7.5 μM acarbose for one hour. The plotted data displays mean responses and error bars represent SD (*n = 3-4*). **P* < 0.05, relative to vehicle control, t test.

Table 1

Modulators of oxygen consumption identified in a screen of 1600 compounds. Oxygen consumption data from the primary screen is presented as fold change from vehicle (FCV) at respective time points in response to 10 μM drug treatment. The strongest activators and inhibitors at 2 hours and the strongest inhibitors at 2 and 24 hours are shown.

	Compound	FCV, 2hrs	FCV, 24hrs
activators	Toltrazuril	2.07 ± 0.83	1.16 ± 0.24*
	Acarbose	1.64 ± 0.51	0.94 ± 0.34*
	Fumazenil	1.59 ± 0.55	1.05 ± 0.34*
	Dichlorophene	1.57 ± 0.32	1.42 ± 0.03
	Nitazoxanide	1.47 ± 0.20	1.27 ± 0.17
	Quinidine Gluconate	1.26 ± 0.05	1.04 ± 0.68*
	Chlormadinone acetate	1.25 ± 0.23	0.45 ± 0.19
	Succinylsulfathiazole	1.20 ± 0.13	0.63 ± 0.34
	Desoxymetasone	1.17 ± 0.19	0.76 ± 0.33
inhibitors	Isoniazid	0.47 ± 0.12	0.33 ± 0.17
	a-Tocopherol	0.51 ± 0.07	0.26 ± 0.12
	Betamethasone Acetate	0.64 ± 0.14	0.38 ± 0.17
	Metaraminol Bitartrate	0.64 ± 0.22	0.51 ± 0.3
	Decoquinate	0.65 ± 0.16	0.36 ± 0.16
	Acamprosate Ca	0.65 ± 0.14	0.36 ± 0.16
	Dyphylline	0.68 ± 0.15	0.38 ± 0.17
	Gallamine Triethiodide	0.71 ± 0.32	0.37 ± 0.13
	Metformin	0.73 ± 0.14	0.60 ± 0.42

FCV = Mean fold change from vehicle

n = 3-4 biological repeats

* not significant at 2±SD at 24 hours only

Table 2

Summary of numbers of modulators of oxygen consumption identified in a screen of 1600 compounds. Numbers are shown for drugs found to be significant in primary screen, compounds that were confirmed upon retest, and drugs that displayed dose-dependent effects on mitochondrial oxygen consumption. Percentage of total number of drugs tested is shown in parentheses.

		1° Screen	Retest Confirmed	Dose Dependent
2 hours	activators	56 (3.5%)	19 (1.2%)	9 (0.6%)
	inhibitors	55 (3.4%)	17 (1.1%)	12 (0.8%)
24 hours	activators	103 (6.4%)	23 (1.4%)	8 (0.5%)
	inhibitors	38 (2.4%)	16 (1%)	12(0.8%)
2 and 24 hours	activators	38 (2.4%)	9 (0.6%)	6 (0.4%)
	inhibitors	21 (1.3%)	15 (0.9%)	11 (0.7%)

Number of significant drugs and percent of total shown